Physica Scripta. Vol. 30, 152–156, 1984

Variable Angle Submillimetre Laser Reflection Spectroscopy of Semiconductors*

P. L. Roselli* and M. W. Evans

Department of Physics, U.C.N.W., Bangor, Gwynedd, Wales, U.K.

J. K. Vij

Department of Microelectronics and Electrical Engineering, Trinity College, Dublin 2, Ireland

and

S. J. Abas

Department of Applied Mathematics, U.C.N.W., Bangor, Gwynedd, Wales, U.K.

Received April 16, 1984; accepted April 28, 1984

Abstract

Power reflection coefficients in σ and π polarisation (R_σ and R_π) have been obtained for silicon type semiconductors doped epitaxially with various concentrations of phosphorous. The coefficients R_σ and R_π are obtained as a function of incidence angle ϕ for disks of semiconductor material doped on one side epitaxially. The $R_\sigma(\phi)$ and $R_\pi(\phi)$ data are reported at four spot frequencies in the far infra-red. These data are not interpretable in terms of the simple band-edge equations of homogenously doped semiconductors in the far infra-red and contain more information than normal angle reflectivity ($\phi = 0$), for which $R_\sigma = R_\pi$. The differences between the measured R_σ and R_π and the values given by the simple homogenous band edge theory vanish as $\sigma \to 90°$, i.e., for glancing angles of incidence. The differences are at a maximum level for $\phi = 0°$, i.e., for normal angles of incidence, especially in σ polarisation, but less so for π polarisation. This suggests that normal incidence reflectivity data probe more deeply into the structure of inhomogenously doped semiconductors or epitaxial layers.

1. Introduction

Reflection spectroscopy has been used extensively in routine characterisation of semiconductor material, but almost always at normal incidence, where the Maxwell equations are easily soluble. For reflection from homogenous semiconductor material we have shown recently [1, 2] that variable angle reflectivity provides new information. If we denote normal incidence by $\phi = 0$ then for $0 < \phi < 90°$ the ratio of reflected energy to incident energy has two components depending on the polarisation of the incoming beam. These two power reflection coefficients are denoted by R_σ and R_π for radiation polarised parallel and perpendicular to the plane of incidence. Near the Brewster angle R_π becomes very small and the reflectivity spectrum is changed greatly with respect to the unpolarised, frequency dependent reflectivity $\phi = 0$. Provided we know the fundamental dependence of R_σ and R_π on ϕ it is possible to obtain more information using variable angle reflectivity then with $\phi = 0$ reflectivity because of the three extra variables ϕ, R_σ and R_π.

* On leave from: Institute of Physics, University of Pisa, Piazza Torricelli, 56100 Pisa, Italy.

2. Theoretical background

The power reflection coefficients R_σ and R_π are defined using Fresnel's formulae and Snell's law, so that:

$$R_\sigma = \frac{a^2 + b^2 - 2a\cos\phi + \cos^2\phi}{a^2 + b^2 + 2a\cos\phi + \cos^2\phi} \tag{1}$$

$$R_\pi = R_\sigma \frac{a^2 + b^2 - 2a\sin\phi\tan\phi + \sin^2\phi\tan^2\phi}{a^2 + b^2 + 2a\sin\phi\tan\phi + \sin^2\phi\tan^2\phi} \tag{2}$$

where

$$a = [\tfrac{1}{2}(\epsilon' - \sin^2\phi) + \tfrac{1}{2}((\epsilon' - \sin^2\phi)^2 + \epsilon''^2)^{1/2}]^{1/2}$$

$$b = \left[\frac{\epsilon''^2}{2(\epsilon' - \sin^2\phi + ((\epsilon' - \sin^2\phi)^2 + \epsilon''^2)^{1/2})}\right]^{1/2}$$

Here ϵ' is the frequency dependent permittivity in the medium and ϵ'' the dielectric loss. For $\phi = 0$ these equations reduce to the more familiar equations of normal reflectivity. The complex permittivity $\epsilon^* = \epsilon' - i\epsilon''$ is of course an intrinsic property of the medium which is being investigated by reflectivity. If the surface and bulk properties of the medium are homogenous (i.e., the same) then in the frequency range of interaction of radiation with free carriers, ϵ^* can be approximated by the well known equation [3]:

$$\epsilon^* = \epsilon_L \left[1 - \frac{(\omega_p \tau)^2}{\omega\tau(\omega\tau - i)}\right] \tag{1}$$

Here

$$\omega_p = \left[\frac{Pq^2}{\epsilon_L m^*}\right]^{1/2} \tag{2}$$

in the plasma frequency, ϵ^* and ϵ_L are the relative permittivities of the homogenous doped and undoped semiconductor, τ is the average relaxation time of free carriers, P is their density (per unit volume); m^* is their effective mass and q the charge on the electron. The permittivity and loss from eqs. (1) and (2) are then:

$$\epsilon' = \epsilon_L \left[1 - \frac{\bar{v}_p^2}{\bar{v}^2 + \bar{v}_e^2}\right] \tag{3}$$

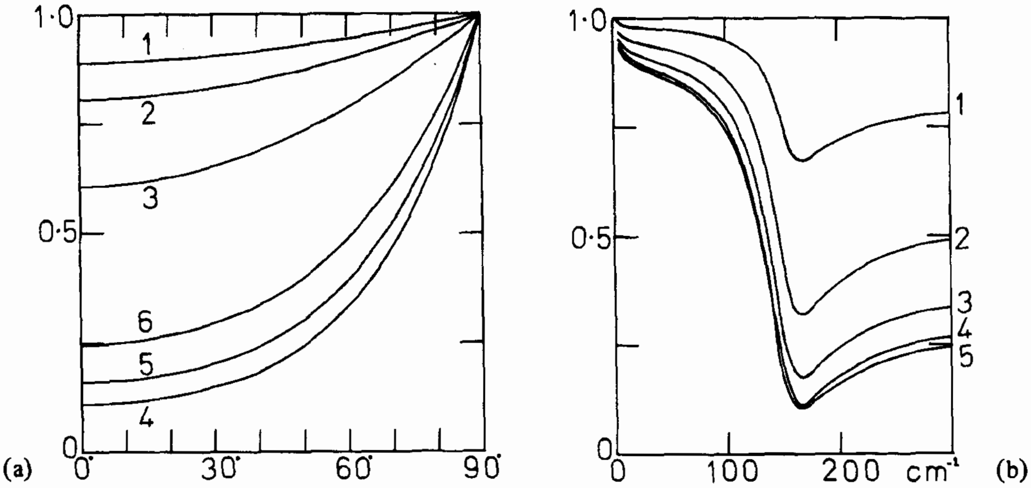

Fig. 1. (a) Plot of power reflection coefficient R_σ from eqs. (3) and (4) vs. incidence angle ϕ for $\epsilon_L = 11.7$; $\bar{v}_p = 150\ \text{cm}^{-1}$; $\bar{v}_e = 220/(2\pi)\ \text{cm}^{-1}$. Normal evidence corresponds to $\phi = 0$. (1) $\bar{v} = 20\ \text{cm}^{-1}$; (2) $80\ \text{cm}^{-1}$; (3) $120\ \text{cm}^{-1}$; (4) $160\ \text{cm}^{-1}$; (5) $200\ \text{cm}^{-1}$; (6) $300\ \text{cm}^{-1}$. *Ordinate* R_σ; *Abscissa*: $\phi°$. (b) Plot of R_σ vs. $\bar{v}$ for (1) $\phi = 80°$; (2) $60°$; (3) $40°$; (4) $20°$; (5) normal incidence.

$$\epsilon'' = \epsilon_L \frac{\bar{v}_e}{\bar{v}} \frac{\bar{v}_p^2}{\bar{v}^2 + \bar{v}_e^2} \tag{4}$$

where $\bar{v}_e = (2\pi\tau c)^{-1}$ is the electron ion collision wavenumber and $\bar{v}_p = \omega_p/2\pi c$ the plasma wavenumber (cm^{-1}).

In these equations the Brewster angle is defined by $\phi_B = \tan^{-1} \epsilon_L^{1/2}$.

R_σ and R_π from these equations are illustrated in Figs. 1 and 2 as functions of $\bar{v}$ and ϕ for a set of test data $\epsilon_L = 11.7$ (*n* type silicon), $\bar{v}_p = 150\ \text{cm}^{-1}$; $\bar{v}_e = 220/(2\pi)\ \text{cm}^{-1}$. An experimentally observed set of reflectivity data must follow self-consistently *all* the various features of Figs. 1 and 2 if eqs. (3) and (4) are really valid.

Variable angle reflectivity is therefore a severe test of the homogeneity of a doped semiconductor sample.

The dependence of R_σ and R_π on wavenumber ($\bar{v}$) (Figs. 1(a) and 2(a)) can be obtained with a spectrometer (grating or interferometer) for various ϕ using, as is this paper, a specular reflectance unit. Their dependence on ϕ at a given $\bar{v}$ (Figs. 1(b) and 2(b)) can be obtained with polarised and collimated laser radiation. This type of spectrum does not seem to be available in the semiconductor literature. If the laser only is used the frequency $\bar{v}_p$ may be identified as the minimum curve $R_\sigma(\phi)$ of Fig. 1(b).

Some useful features of the spectra in Figs. 1 and 2 may be identified as follows.

(i) The curve $R_\pi(\bar{v})$ (Fig. 2(a)) *changes shape above the Brewster angle* $\phi_p = \tan^{-1} \epsilon_L^{1/2}$.

If a given semiconductor sample is truly homogenous (eqs. (3) and (4)) this shape-change, seen theoretically in Fig. 2(a) must also be observable experimentally, together with all the other features of Figs. 1 and 2.

(ii) The $R_\sigma(\phi)$ and $R_\pi(\phi)$ curves (Figs. 1(b) and 2(b)) are different in appearance for $0 < \phi < 90°$ but identical at $\phi = 0$ (normal reflectivity) and $\phi = 90°$, when the laser beam is parallel to the surface of the sample. The $R_\sigma(\phi)$ curves are monotonic increasing functions whereas $R_\pi(\phi)$ shows minima. The position (in terms of ϕ) and depth of these minima change greatly with ϕ and $\bar{v}$. As $\bar{v} \to 0$ (Fig. 2(b)) the minimum becomes infinitely sharp and shifts infinitesimally near $\phi = 90°$. This does not occur at all in σ polarisation.

None of these features, obtained by varying ϕ, seem to have been reported previously in the solid-state literature. We mention in passing that similar features would be observable in highly absorbing liquids such as water or the alcohols, in the far infra-red frequency region [4].

Reflectivity spectra at normal incidence ($\phi = 0$) are known

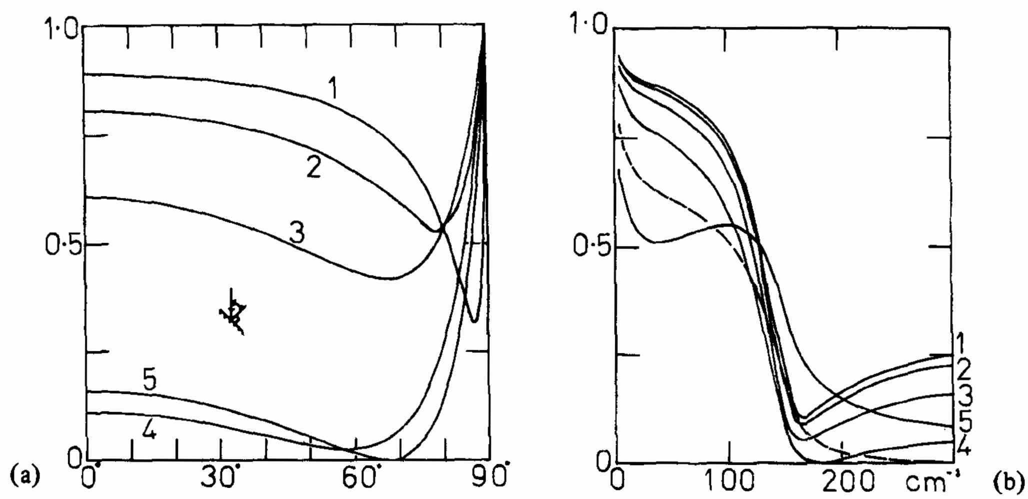

Fig. 2. (a) As for Fig. 1(a), R_π vs. ϕ; (1) $20\ \text{cm}^{-1}$; (2) $80\ \text{cm}^{-1}$; (3) $120\ \text{cm}^{-1}$; (4) $160\ \text{cm}^{-1}$; (5) $200\ \text{cm}^{-1}$. (b) As for Fig. 1(b): R_π vs. $\bar{v}$; (1) $\phi = 0°$; (2) $20°$; (3) $40°$; (4) $60°$; (5) $80°$; – – – – –, Brewster angle, $\phi = 73.5°$.

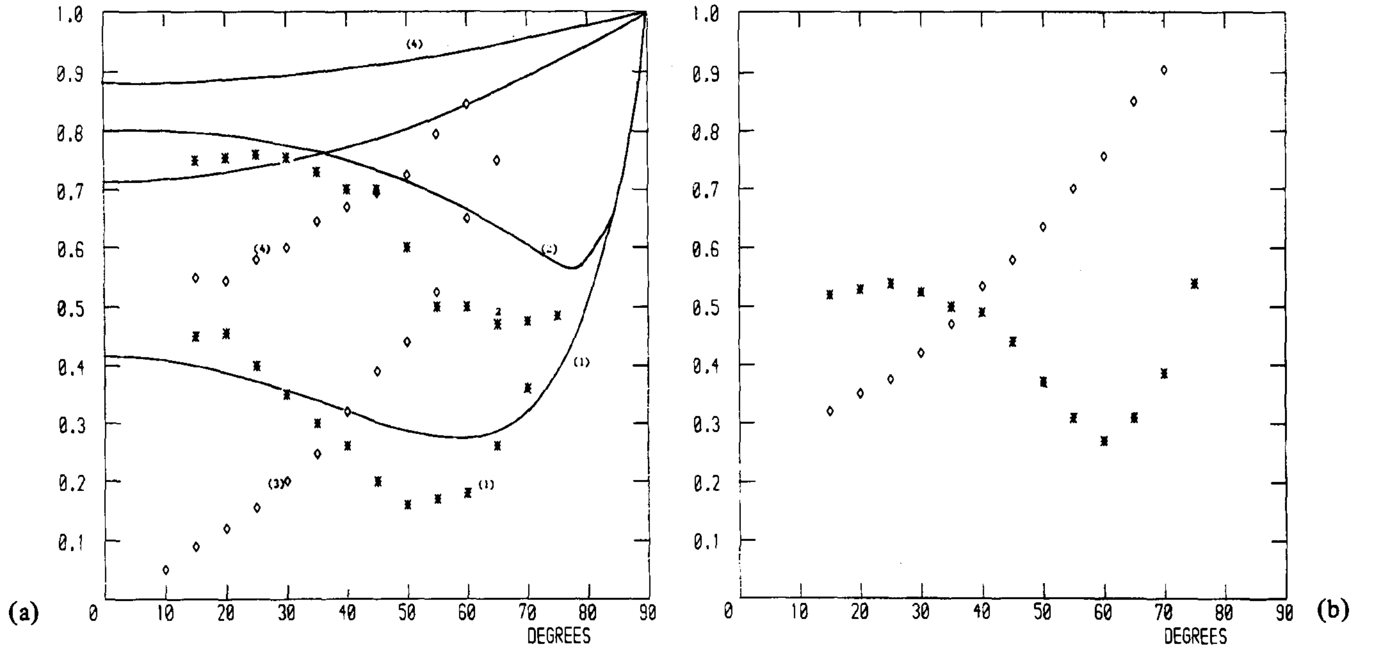

Fig. 3. (a) Experimental reflectivity data for the machined side of sample 3. *, (1) R_π at $131\,cm^{-1}$; (2) R_π at $84\,cm^{-1}$; (3) ◇, R_σ at $104\,cm^{-1}$; (4) ◇, R_σ at $40\,cm^{-1}$. ——— (1) Least mean squares best fit of eqs. (3) and (4) to R_π at $131\,cm^{-1}$, $\bar{\nu}_p = 143\,cm^{-1}$. ——— (2) to (4) R_π and R_σ curves at 84, 104 and $40\,cm^{-1}$ generated by this l.m.s. best fit. (b) *, R_π at $131\,cm^{-1}$; ◇, R_σ at $104\,cm^{-1}$, substrate.

to change in appearance when the sample is inhomogenous, or for epitaxial layers. The relevant Maxwell equations in this case have been solved by Hild and Grofscik [5]. The solution of these Maxwell equations for $\phi > 0$ seems to be unknown, but seems also to be of critical importance in the study of inhomogenous semiconductors and epitaxial layers, because of the various depths of sample seen by the laser beam for various angles of ϕ.

3. Experimental method

Reflectivity spectra $R_\sigma(\phi)$ and $R_\pi(\phi)$ were obtained with an Apollo Instruments tunable submillimetre laser and an Analytical Accessories specular reflectance unit. σ polarisation was used at $40\,cm^{-1}$ and $104\,cm^{-1}$, and π polarisation at $84\,cm^{-1}$ and $131\,cm^{-1}$. The complete laser system is fully described elsewhere [6]. The output signal from the specular reflectance unit is detected by a Golay pneumatic cell and amplified using internal electronic modulation of the pump CO_2 laser. In this work the signal was detected with an oscilloscope. Alternatively it is possible to use a lock-in amplifier when the laser output is weak or fluctuates in intensity.

Power reflection coefficients R_σ and R_π were measured using the ratio of the oscilloscope signal from the sample (epitaxial layer and substrate) to a background reflecting mirror supplied by Analytical Accessories Ltd., as part of the specular reflectance unit. This unit uses a separate parabaloid mirror and in consequence the background signal is at a constant with varying ϕ. This instrumental function is removed in the ratios. The specular reflectance unit is effective between $\phi = 20 \pm 2^\circ$ and $\phi = 70 \pm 2^\circ$. Above and below these angles the signal is cut off by the geometry of the optical configuration used. The system could, therefore, be simplified and improved.

4. Sample preparation

The doped semiconductor samples used were prepared by gas–solid epitaxy at Philips of Eindhoven, Netherlands. The substrate (intrinsic semiconductor) was n^+ type Si, about $200\,\mu m$ thick. These wafers were heated in a furnace in the presence of phosphine gas and Si added epitaxially to a depth of approximately $50\,\mu m$, to form an n/n^+ junction at the interface. The

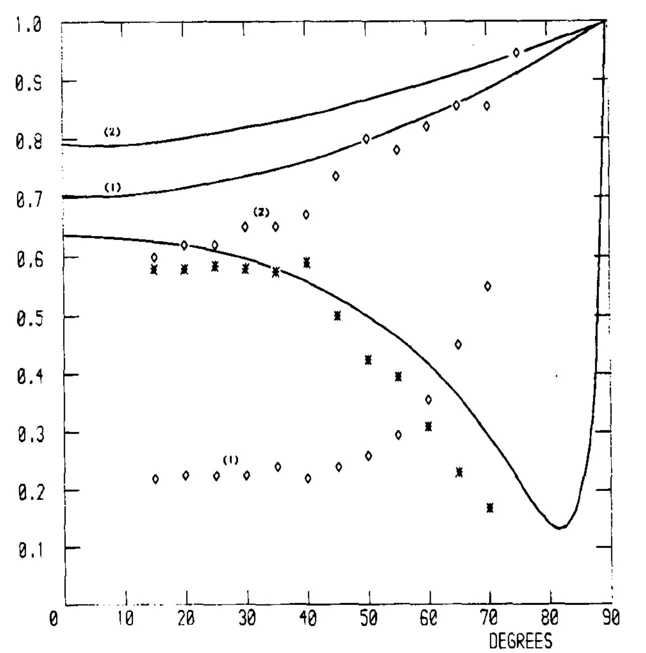

Fig. 4. Substrate of sample 2. *, R_π at $131\,cm^{-1}$; ◇, (1); R_σ at $40\,cm^{-1}$, (2) R_σ at $84\,cm^{-1}$. ———, Least mean squares best fit to R_π of eqs. (3) and (4), $\bar{\nu}_p = 951\,cm^{-1}$. ———, (1) and (2) R_σ at $40\,cm^{-1}$ and $84\,cm^{-1}$ respectively generated by the fit to R_π at $131\,cm^{-1}$.

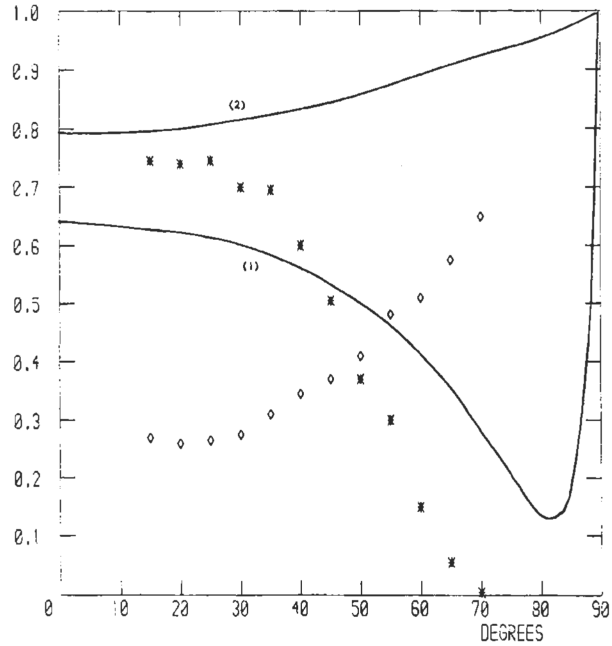

Fig. 5. Machined side of sample 5. *, (1) R_π at 131 cm^{-1}; (2) ◇, R_σ at 40 cm^{-1}. ———, (1) L.m.s. best fit of eqs. (3) and (4) to R_π $\bar{\nu}_p = 987$ cm^{-1}. ———, (2) R_σ at 40 cm^{-1} generated by this fit.

epitaxial (n) side of the wafer was machined and polished. The effective electron mass in these wafers is a tensor quantity, ranging from about 0.2 to about 0.98 of the electron mass [7]. The epitaxial and uncoated sides of these samples showed very different R_σ and R_π behaviour, except for sample 5.

5. Results and discussion

Power reflection coefficients R_σ and R_π for different samples are shown in Figs. 3–5 respectively. The general dependence of R_σ and R_π upon ϕ is similar to that in Figs. 1 and 2, i.e., $R_\sigma(\phi)$ is a monotonic increasing function and $R_\pi(\phi)$ shows minima which shift with wavenumber ($\bar{\nu}$). $R(\phi = 0)$ as a function of $\bar{\nu}$ is the standard, normal incidence, reflectivity spectrum.

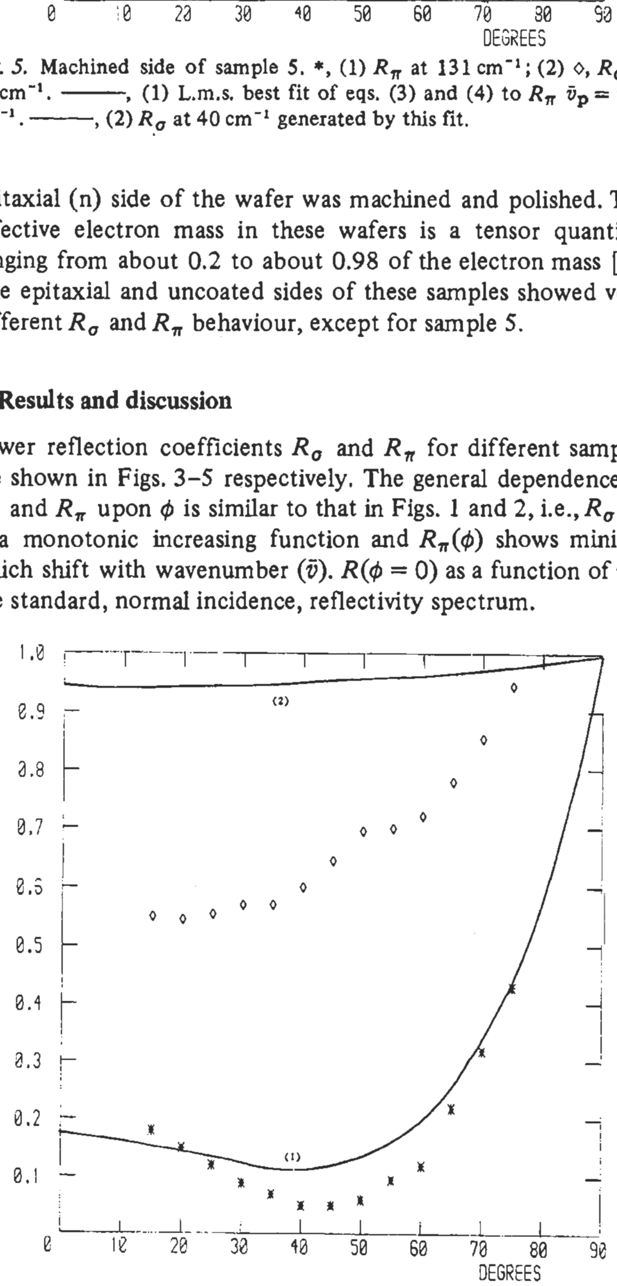

Fig. 6. As for Fig. 5, machined side of sample 4. $\bar{\nu}_p = 131$ cm^{-1}.

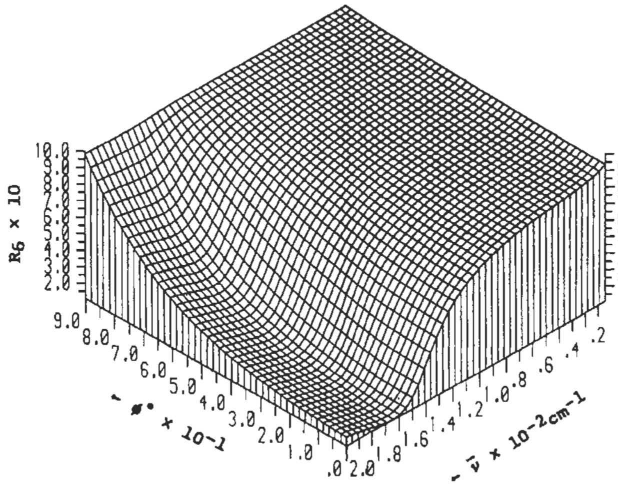

Fig. 7. $R_\sigma(\phi, \bar{\nu})$ for $\bar{\nu}_p = 150$ cm^{-1}, $\bar{\nu}_e = 110/\pi$ cm^{-1}.

However, a detailed analysis of the spectra of Figs. 3–6 with eqs. (3) and (4) quickly reveals that the submillimetre variable ϕ spectra are not those of homogenously doped semiconductors. This is true of both the epitaxial layer and substrate in the semiconductor samples. For example, in machined side of sample 3 (Fig. 3(a)) it is clear that the minimum of the standard $\phi = 0°$ spectrum is near 104 cm^{-1}, but this is preceded by a *maximum* near 84 cm^{-1}, suggesting that there are interference fringes in the spectrum of the type described by Hild and Grofscik [5] for epitaxial layers or otherwise inhomogenously doped semiconductors. We have force-fitted eqs. (3) and (4) to R_π at 131 cm^{-1} with a least mean squares non-linear Gauss–Newton minimisation program (N.A.G.E04FAA) keeping $\epsilon_L = 11.7$ (n type silicon) and iterating on $\bar{\nu}_p$ and $\bar{\nu}_e$. This gives $\bar{\nu}_p = 143$ cm^{-1}, $\bar{\nu}_e = 30$ cm^{-1}; a result which is clearly high with respect to the low R_σ curve at 104 cm^{-1}. It is clear from the theoretical l.m.s. force-fit in Fig. 3(a) that eqs. (3) and (4) at $\phi = 0$ give a straightforward "homogenous" type $R(\bar{\nu})$ spectrum at $\phi = 0$, i.e., decreasing monotonically from $\bar{\nu} = 40$ cm^{-1} to 131 cm^{-1}, with a minimum near 143 cm^{-1} ($= \bar{\nu}_p$, theoretical).

The reflectivity spectrum of the substrate (Fig. 3(b)) shows similar features to that of the epitaxial layer, i.e., the R_σ curve is monotonic increasing and the R_π shows a minimum near 60°. Again, this type of variable angle reflectivity spectrum cannot

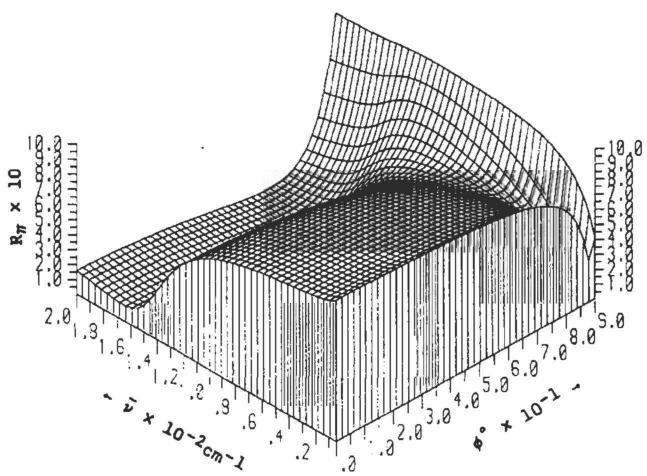

Fig. 8. $R_\pi(\phi, \bar{\nu})$ for $\bar{\nu}_p = 150$ cm^{-1}, $\bar{\nu}_e = 110/\pi$ cm^{-1}.

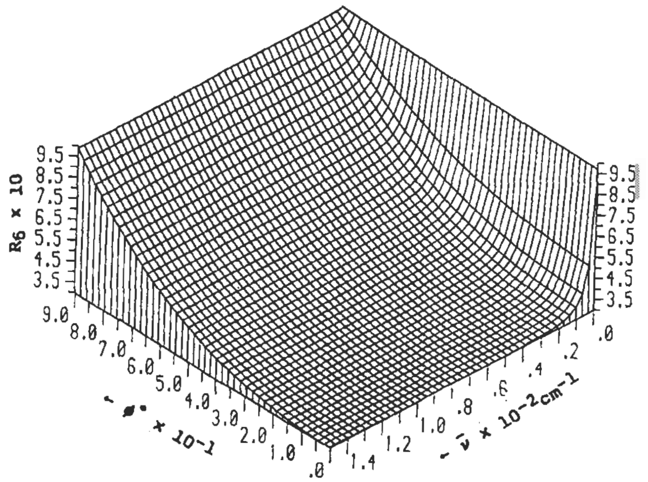

Fig. 9. $R_\sigma(\phi, \bar{\nu})$ for $\bar{\nu}_p = 4.2\ \mathrm{cm}^{-1}$, $\bar{\nu}_e = 23.92\ \mathrm{cm}^{-1}$.

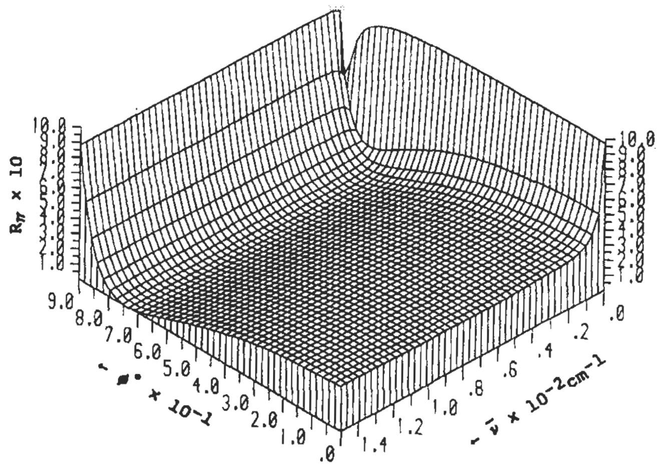

Fig. 10. $R_\pi(\phi, \bar{\nu})$ for $\bar{\nu}_p = 4.2\ \mathrm{cm}^{-1}$, $\bar{\nu}_e = 23.92\ \mathrm{cm}^{-1}$

be described by the standard semiconductor equations. However, it is possible to say that the epitaxial layer is relatively lightly doped, because of the similarity of the R_σ and R_π coefficients on both sides of the sample.

In the substrate of sample 2, on the other hand (Fig. 4), a least mean squares force fit of the semiconductor equations provides $\bar{\nu}_p = 950\ \mathrm{cm}^{-1}$, $\bar{\nu}_e = 1800\ \mathrm{cm}^{-1}$, but again the resulting R_σ curves are grossly at odds with the experimental data, probably indicating the presence of fringes [5] caused by the concentration gradient at the epitaxial/substrate junction. The situation is similar in sample 5, where $\bar{\nu}_p = 987\ \mathrm{cm}^{-1}$, indicating that the carrier concentration is in the range $10^{19}\ \mathrm{cm}^{-3}$ (Fig. 5).

In contrast, the machined side of sample 4 is relatively lightly doped ($\bar{\nu}_p = 131\ \mathrm{cm}^{-1}$), with a well-defined minimum in the R_π curve at $131\ \mathrm{cm}^{-1}$ (Fig. 6). The best fitting again produces an R_σ curve at $40\ \mathrm{cm}^{-1}$ which differs considerably from the experimental data, indicating once more the approximate nature of eqs. (1) and (2) as a description of these epitaxial samples.

Power reflection spectroscopy is, therefore, a powerful means of investigating the nature of simple semiconductor material investigating even when we have available, as in this case, only a few spot frequencies in the far infra-red. Broad-band variable angle R_σ and R_π data would be very useful in the study of epitaxial layer/substrate properties and depth profiles.

Finally in Figs. 7–10 we have plotted R_σ and R_π as a function of incidence angle ϕ and wavenumber, $\bar{\nu}$. These surface plots illustrate the amount of information available, in principle, from reflectivity experiments on semiconductor samples in the far infra-red, using a combination of laser and broad-band spectroscopy.

Acknowledgements

The University of Wales is thanked for a Fellowship, and the Nuffield Foundation for a bursary to PLR.

References

1. Evans, M. W., J. Chem. Soc., Faraday Trans. II 76, 1147 (1980).
2. Evans, M. W., Adv. Mol. Rel. Int. Proc. 16, 227 (1980).
3. E.g., Chantry, G. W., Submillimetre Spectroscopy. Academic, New York (1971).
4. Evans, M. W., Evans, G. J., Coffey, W. T. and Grigolini, P., Molecular Dynamics. Wiley/Interscience, New York (1982).
5. Hild, E. and Grofcsik, A., Infra-red Physics 18, 23 (1978).
6. Reid, C. J., Spectrochim. Acta 38A, 697 (1982).
7. Scaife, B. K. P., Communication.